ARTICLE

A New Three-Dimensional (3D) Printing Prepress Algorithm for Simulation of Planned Surgery for Congenital Heart Disease

Vitaliy Suvorov[1,2,*], Olga Loboda[2], Maria Balakina[1] and Igor Kulczycki[2]

[1]Department of Surgical Diseases of Children, Saint Petersburg State Pediatric Medical University, Saint Petersburg, Russia

[2]Higher School of Theoretical Mechanics, Peter the Great Saint Petersburg Polytechnic University, Saint Petersburg, Russia

*Corresponding Author: Vitaliy Suvorov. Email: vitalikkrak@gmail.com

ABSTRACT

Background: Three-dimensional printing technology may become a key factor in transforming clinical practice and in significant improvement of treatment outcomes. The introduction of this technique into pediatric cardiac surgery will allow us to study features of the anatomy and spatial relations of a defect and to simulate the optimal surgical repair on a printed model in every individual case. **Methods:** We performed the prospective cohort study which included 29 children with congenital heart defects. The hearts and the great vessels were modeled and printed out. Measurements of the same cardiac areas were taken in the same planes and points at multislice computed tomography images (group 1) and on printed 3D models of the hearts (group 2). Pre-printing treatment of the multislice computed tomography data and 3D model preparation were performed according to a newly developed algorithm. **Results:** The measurements taken on the 3D-printed cardiac models and the tomographic images did not differ significantly, which allowed us to conclude that the models were highly accurate and informative. The new algorithm greatly simplifies and speeds up the preparation of a 3D model for printing, while maintaining high accuracy and level of detail. **Conclusions:** The 3D-printed models provide an accurate preoperative assessment of the anatomy of a defect in each case. The new algorithm has several important advantages over other available programs. They enable the development of customized preliminary plans for surgical repair of each specific complex congenital heart disease, predict possible issues, determine the optimal surgical tactics, and significantly improve surgical outcomes.

KEYWORDS

3D printing; imaging in cardiac surgery; congenital heart disease; modelling in cardiac surgery; pediatric cardiology; algorithmic modelling of the heart; medical imaging; 3D modelling

1 Introduction

3D printing is a widely used technique that has recently found its way into the medical industry. It has become an increasingly popular tool that contributes to rapid technological progress. Along with the increasing availability of 3D printing, this tool has also begun to be used in medical practice to improve methods of surgical repair for various pathologies [1,2]. Current technologies allow professionals to obtain virtual 3D reconstructions of any part of the body to acquire an accurate image of a pathology,

organ arrangement, and tumor localization [2,3]. At the moment, most of the studies on the use of 3D printing in medicine belong to reconstructive, cancer, and maxillofacial surgery [4–11]. Tack et al. analyzed 227 surgical papers and found that their outcomes demonstrated the advantages of using organ models for the assessment of anatomy and pathology obtained by 3D printing technology as compared to traditional imaging tools in medicine [12]. Application of this method in maxillofacial surgery, traumatology, and orthopedics improved the outcomes of plastic and reconstructive surgeries, while in other areas of surgery, such as hepatic surgery or cardiac surgery 3D printing has been actively used over the past few years [13–17].

In recent years, 3D printing technology has improved significantly and become more affordable. Manufacturing a parenchymal and/or a hollow organ primarily focuses on the internal areas, for example, ventricular septum defects, and its localization in relation to the great vessels [15,18]. In reconstructing bone structures, the most important is to focus on its outer borders. An interesting study was carried out in cancer surgery, which proved that 3D printing reduced operating time, blood loss, shortened postoperative recovery period, and improved the accuracy of manipulations [19].

Nevertheless, it can be difficult to assess the spatial relations between structures such as intracardiac defects, coronary arteries, or other formations [18,20]. It is necessary to premeditate the best strategy for surgical repair. In cardiovascular surgery, 3D printing has been practiced and progressively implemented for the last ten years, as evidenced by the increased number of publications, most of which were clinical cases, applied in the treatment of adult patients [16,21]. One should notice increasing interest among cardiac specialists in the use of 3D printing in pediatric cardiac surgery.

In their systematic review, Wang et al. analyzed 43 publications on 3D modeling in adult cardiac surgery and reported better accuracy of visualization of complex anatomy, benefits of 3D modeling in preoperative planning, and prediction of intraoperative issues [22]. The high diagnostic significance of the method was noted. It should also be noted that among 43 analyzed papers, only 6 studies included more than 10 patients. One more study showed the high value of 3D models for the training of surgeons in the preclinical development of new devices [23]. A recent study reported successful 3D printing of an aortic stenosis model with realistically fragile and destructible calcifications in order to train beginner surgeons [24].

According to some studies, 3D printing in pediatric cardiac surgery may also be effectively used [20,25]. This method of visualization may improve the outcomes of surgical repair, as it makes it possible to assess the spatial relations of organs, structures, and formations. It will allow a reduction in the risk of adverse events caused by manipulations in the surgical field. The more complex the anatomical region and the smaller the size of its structures, defects, and formations are, the more challenging it is to plan every stage of the procedure. Having an identical real-sized anatomical model makes the chance of avoiding adverse events during surgery remarkably higher; since it becomes possible to accurately assess both sizes of structures and their interrelation and connections.

A number of publications note that printed heart models are more informative than virtual 3D visualization methods [26]. Valverde et al. believed that 3D-printed models in preoperative planning can significantly improve the quality of complex surgical procedures, such as the Nikaidoh procedure in patients with transposition of the great arteries and left ventricular outflow tract obstruction [20].

The rapid development of 3D printing technique in various areas of surgery for preoperative preparation, as well as for studying features of topographic anatomy of a pathology and for reduction of the risk of intraoperative complications, advanced this method and promoted its implementation, in pediatric cardiac surgery in particular [20,27]. Considering the complexity and variability of most congenital heart defects, it is important to have high detail accuracy when printing cardiac models. Such requirements are

determined due to a small step in the measurement of anatomical defects, and anomalies, in contrast to those in adult cardiac surgery. In addition, we consider it promising to develop this method not only for planning an option for surgical repair but also for simulation of the selected procedure on a printed heart in each individual case. Therefore, in our study, the main task was to compare measurements of anatomical zones on a printed cardiac model with similar areas on computed tomography.

In recent years, multislice computed tomography (MSCT), magnetic resonance imaging (MRI), single photon emission computed tomography, echocardiography, and other imaging technologies have gradually developed and are widely used not only for diagnostic purposes but also for the conversion of digital data into virtual and physical 3D models [28–30]. Computed tomography data were used for our study. One of the challenges in manufacturing a physical model of the heart and great vessels is the need to model the object using MSCT data for subsequent printing. On the one hand, this process requires a specialist who has the skills to work with 3D modeling software, to post-process the printed model, a specialist with knowledge and experience. Besides, this stage of manufacturing a three-dimensional cardiac model takes at least 2–3 h [13]. On the other hand, the stage of preparation (especially segmentation) of a cardiac model or any other organ requires knowledge of the anatomy of a defect or pathology, since the information content of the printed three-dimensional model directly depends on this. Given these features of computed tomography data processing, one of the goals of this study was to develop a new preprinting algorithm that would simplify and speed up the preparation of a three-dimensional model for printing, while maintaining high accuracy and detail degree. The objective of this study was to evaluate the efficiency of the new algorithm for the preparation of cardiac models with congenital defects for 3D printing.

2 Materials and Methods

Prospective cohort study was performed from May 2020 to December 2021. To carry out this single center study we modelled and printed out the hearts and great vessels of 29 children with congenital heart defects, 26 of which were newborns treated at the clinic of St. Petersburg State Pediatric Medical University. The patients were divided into 2 equal groups. Our study was approved by the ethics committee (the local ethics committee at Saint Petersburg State Pediatric Medical University, No. 18/03 27.10.2022). Parents of the patients were informed about the use of the examination and treatment data for scientific research and gave their consent.

As a part of preoperative examination, all patients underwent contrasted chest organ MSCT on a Philips Ingenuity 128 Slice machine with intravenous contrast agent Optiray 300 (Ioversol), with synchronization according to the ECG signal. The study was performed according to the standard technique, using cardiac gating, followed by the construction of multiplanar reformations. Intravenous bolus administration of a non-ionic isoosmolar contrast agent in a volume of 1.5–2 ml/kg was carried out using an automatic two-flask syringe-injector. The rate of administration of the radiopaque preparation varied within 0.5–1.0 ml/s.

The obtained data are usually processed using open-source medical software packages such as 3D slicer. In our study, new algorithm for preparation of heart models for 3D printing was used to process tomography data and obtain a virtual 3D model. This step is performed automatically. Upon its completion, it is necessary to perform model validation and, if necessary, additional segmentation. By processing DICOM files, a three-dimensional model of the heart and great vessels was obtained in .STL or .OBJ format. As usually the resulting model has extra surfaces and irregularities caused by noise effects during MSCT, the model was filtered using the Meshmixer program (ver. 3.5.474) and prepared for printing on a 3D printer. The model was printed using photopolymers on a 3D printer (Creality Halot Sky) in compliance with the dimensions of the printed model to the actual dimensions of the heart and great vessels 1:1 (Fig. 1).
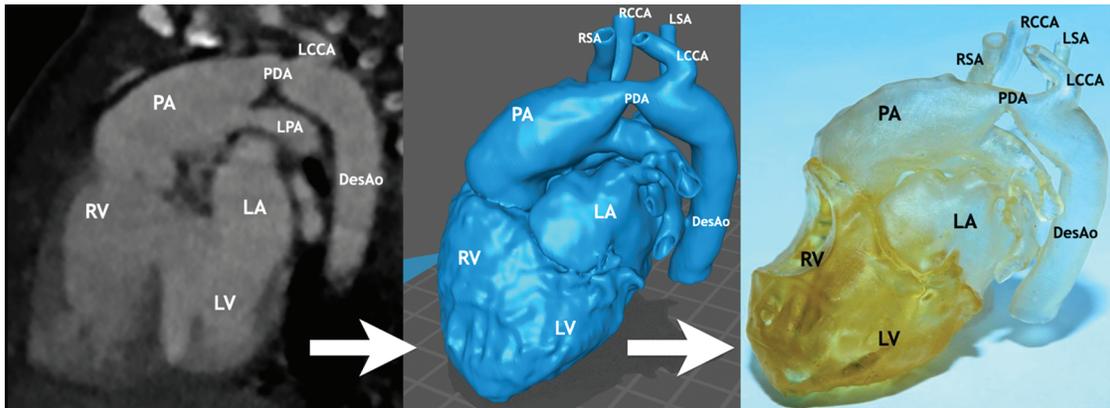
Figure 1: Stages of preparation for 3D printing of the heart and great vessels of a child with interrupted aortic arch (type C). The method consisted of three steps: I—obtaining digital images—slices of computed tomography, II—the stage of data processing and segmentation of anatomical zones with obtaining a virtual model for printing, and III—printing the 3D heart model. Notes: RV, right ventricle; LV, left ventricle; PA, pulmonary artery; LA, left atrium; LPA, left pulmonary artery; PDA, patent ductus arteriosus; DesAo, descending aorta; RCCA, right common carotid artery; RSA, right subclavian artery; LCCA, left common carotid artery; LSA, left subclavian artery

2.1 MSCT Data Processing Using the New Developed Algorithm

2.1.1 Pre-Processing

The Python library PyDicom was used to process CT images [31]. This library allows to fully read the .dcm files and works with information stored in the images. And for fast work with information of images the library NumPy was used. To work conveniently and easily with the snapshots, normalization must be carried out, i.e., so that all the values of the snapshot numbers are always only in the same range. This is done by multiplying each value by a certain factor. This process will reduce the values of the series of snapshots to a convenient form, in this case reduced to an 8-bit number, i.e., from 0 to 255. The contrast ratio parameter is chosen experimentally, however. To simplify image processing and the subsequent finding of the heart border, it may be convenient to use the rate of change of values or even the rate of change, i.e., $\Delta A_{i,j,k}$. A Kenny detector can help to detect boundaries. The Kenny detector (Kenny operator, Kenny algorithm) is an algorithm for detecting object boundaries in an image. This algorithm is implemented in the OpenCV library. In the work, boundary search methods were combined. To increase the speed of the program it is necessary to carry out optimization at each stage, including reduction of the processing area. Prir to full image processing, it is necessary to determine in what area of the 3D image the body of interest, in this case the heart, is located. The range of number values should also be determined at this stage so that the heart tissue can be clearly distinguished from other tissues, including bone. To reduce the amount of image processing, software image cropping was carried out.

2.1.2 Complete Processing

Complete processing means preparation of images for further 3D body development. It requires the initial processing parameters that were obtained during the previous step: volume and range. As well as a properly selected parameters that, based on this data, will perform a full processing of the image: leaving out the areas belonging to the heart. It is crucially important to highlight areas where material, i.e., heart tissue, is or is not present in the images, so that the 3D object can be constructed in a qualitative manner later. The OpenCV library can help to find the contours of the object. To find areas of the inner shell, images with contrast must be used; the contrast makes it possible to see all the shells and boundaries of the inner lining of the heart. As the contrast only touches the inner shell of the heart and does not

penetrate the tissue, it allows the internal structure of the heart to be highlighted. To determine the correct range of numbers to minimize error in the model, the practicing cardiovascular surgeon identifies what areas of the scan belong to the heart and which do not, as well as what pathology in the heart is visualized.

For the outer shell, the range of number values must be defined very precisely so that the maximum number of outer borders can "stand out" in the images. In this case, it is better to use images with contrast. Because, even if the outer boundary is not visible, it can be reconstructed much easier from these images. It may also be the case that voids may appear in the images inside a solid object.

2.1.3 Marching Cubes

After all the images were processed, a record was made into a separate 3D matrix, which in its turn had already been entered into a separate algorithm that created the 3D model. A common algorithm for this kind of problem, such as Marching Cubes, was used to construct the 3D object [32]. The code for this algorithm was taken from the public domain [33].

2.1.4 Post-Processing

Afterwards, the results had to be processed. When using the marching cubes algorithm, all polygons remain independent. To solve this problem, the marching cubes algorithm was rewritten in C++ and post-processing was added. The following things are now automated:

–Deletion of recurring vertices;

–Filling voids;

–Smoothing.

To perform the study, measurements were taken of similar areas in the same planes and points on MSCT images and on a printed model of the heart and great vessels, in connection with which 2 groups were formed: group 1 with measurements on computed tomography images, group 2—on 3D models [34]. Measurements were taken by two observers. A digital caliper was used to measure the models. The measurements were carried out at the following points: the length of the heart was measured from the apex to the most distant point of the right atrium; the width of the heart—in the projection of the coronary sulcus; at a distance of 1 cm from the fibrous ring of the aortic and pulmonary valves, the diameter of the ascending aorta and pulmonary artery, respectively, was assessed; at a distance of 0.5 cm from the bifurcation of the pulmonary trunk, the diameter of the right and left pulmonary arteries was assessed; the diameter of the brachiocephalic trunk (BCT), the left common carotid artery (LCCA) and the subclavian artery (LSA) was determined at a distance of 0.5 cm from the aortic arch; the diameter of the aortic arch (segment C) was measured between the BCT and the LCCA; at a distance of 0.5 cm after LSA, the diameter of the descending aorta was calculated. The diameter of the patent ductus arteriosus (PDA) was evaluated by the smallest dimension.

2.2 Statistical Analysis

The differences between the 2 groups were compared using independent samples t-tests for the continuous variables with normal distributions, Mann–Whitney U-test in case of abnormal distributions. Statistical processing was carried out using SPSS for Windows. The level of statistical significance is accepted for $p < 0.05$.

3 Results

To perform this study we analyzed 29 pediatric cases, 26 of whom were newborns with various types of CHD. The mean age of the patients at the time of surgery was 88.7 days (minimum—2 days, maximum—537 days). The average weight was 4424 g (minimum—2000 g, maximum—12000 g). The time spent processing data and preparing a model for 3D printing using the new algorithm is no more than 10 min (minimum—2 min, maximum—10 min). A more detailed description of patients is presented in Table 1.

Table 1: Demographic and clinical characteristics of the patients

Characteristics	1 group* (n/%)	2 group* (n/%)	p-value
Total number of patients	29/100	29/100	–
Demographic and clinical characteristics			
Sex (male)	15/51.7	15/51.7	–
Age at the time of surgery, days (mean/SD)	88.7/146.3	88.7/146.3	–
Weight, g	4424/2429	4424/2429	–
Neonate	26/89.7	26/89.7	–
Type of CHD:			–
AVSD, complete unbalanced form	1/3.5	1/3.5	
Pulmonary atresia type 1, SV, heterotaxy	1/3.5	1/3.5	
DORV (Taussig-Bing anomaly)	2/6.9	2/6.9	
VSD (apical, non-restrictive)	1/3.5	1/3.5	
HLHC	3/10.3	3/10.3	
CoA, aortic arch hypoplasia, with/without VSD	7/24.1	7/24.1	
TA, type 1A	1/3.5	1/3.5	
IAA, type C	2/6.9	2/6.9	
Sling of the LPA	1/3.5	1/3.5	
VR, complete form in 2 patients (6.9%);	2/6.9	2/6.9	
StPA (subvalvular) severe, SV, heterotaxy	1/3.5	1/3.5	
TAPVR	2/6.9	2/6.9	
D-TGA with/without VSD	4/13.8	4/13.8	
ccTGA, DORV, AVSD, complete balanced form	1/3.5	1/3.5	
Measurement results			
Heart length, mm (Md)	57.7 [54.5; 66.2]	60 [54.8; 65.9]	0.65
Heart width, mm (Md)	41.4 [38; 46.7]	41.8 [37; 46.8]	0.98
D PA, mm (mean/SD)	10.1/3.3	10.5/3.5	0.64
D RPA, mm (mean/SD)	5.6/2.1	5.8/2.1	0.64
D LPA, mm (mean/SD)	5.3/2.3	5.7/2.3	0.49
D AscAo, mm (mean/SD)	7.9/2.5	8.5/2.5	0.45
D AoArch, mm (Md)	6.1 [4.8; 7.5]	5.8 [4.5; 7.4]	0.52
D BCT, mm (mean/SD)	4.8/1	5.3/1.2	0.1
D LCCA, mm (mean/SD)	3.7/0.9	3.9/1	0.26
D LSA, mm (mean/SD)	3.6/1	3.9/1	0.27
D DesAo, mm (mean/SD)	6.3/1.6	6.8/1.7	0.31

Notes: 1 group*: CT-scan; 2 group*: 3D-model. CHD, congenital heart disease; AVSD, atrioventricular septal defect; SV, single ventricle; DORV, double-outlet right ventricle; VSD, ventricular septal defect; HLHC, hypoplastic left heart complex; CoA, coarctation of the aorta; TA, truncus arteriosus; IAA, interrupted aortic arch; LPA, left pulmonary artery; VR, vascular ring; StPA, stenosis of the pulmonary artery; TAPVR, total anomalous pulmonary venous return; D-TGA, D-transposition of the great arteries; ccTGA, congenitally corrected transposition of the great arteries; D, diameter; PA, pulmonary artery; RPA, LPA, right and left pulmonary arteries; AscAo, ascending aorta; AoArch, aortic arch; BCT, brachiocephalic trunk; LCCA, left common carotid artery; LSA, left subclavian artery; DesAo, descending aorta.

3.1 Comparison of Measurements on Similar Areas of CT Images and on a Printed Models

As a result of our study, comparisons were made of similar areas on a tomography image and on 3D printed models of the heart and great vessels of children with congenital heart disease. Fig. 2 shows an example of this stage of the study in a child with hypoplastic left heart syndrome (mitral valve hypoplasia, left ventricular hypoplasia, ascending aorta and aortic arch hypoplasia, dilated pulmonary artery).
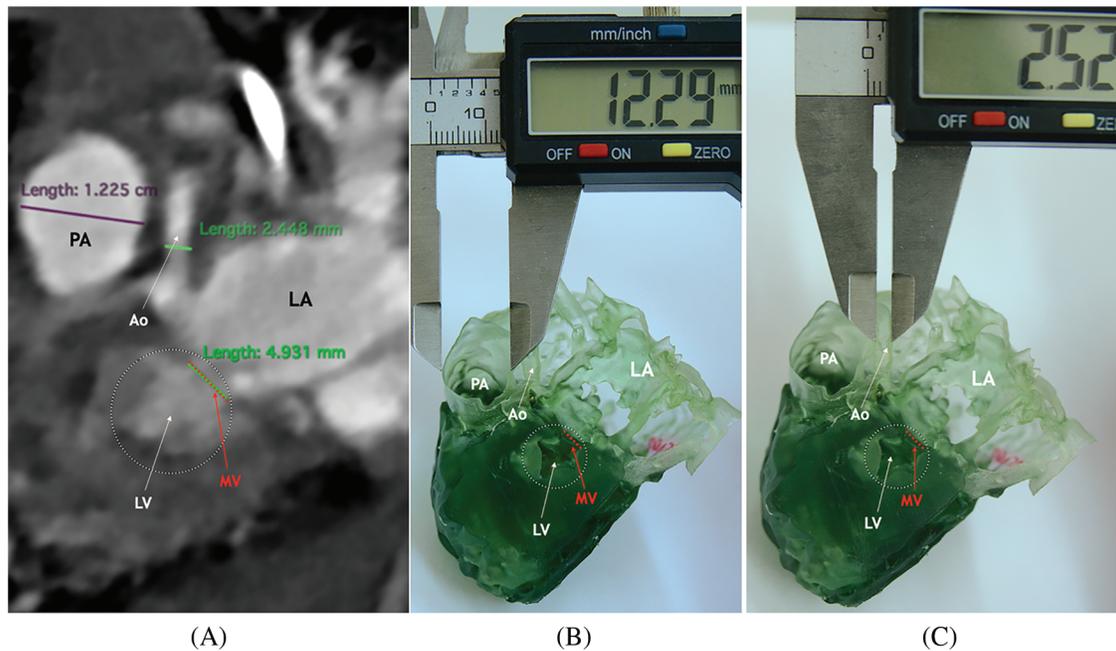

Figure 2: Comparison of measurements on similar areas of CT images and on a printed model in a child with hypoplastic left heart syndrome. CT-scan image (A) and 3D printed model (B), (C) of a heart cut longitudinally. Notes: LV, left ventricle; PA, pulmonary artery; LA, left atrium; MV, mitral valve; Ao, ascending aorta

Measurements of 29 cases were obtained and analyzed using statistical methods. The results of a statistical analysis of comparison of measurements of similar areas on a printed three-dimensional model and according to MSCT data of the heart and great vessels are presented in Tables 2 and 3. According to the result of the statistical analysis of the data, the measurements on the three-dimensional printed model of the heart and on the computed tomography images did not differ statistically significantly, which allowed us to conclude that the model was highly accurate and informative.

Table 2: Statistical analysis results for measurement comparison (independent samples t-test)

Measurement area	M/SD		t	CI [95%]	p^1
	1 group*	2 group*			
D PA	10.1/3.3	10.5/3.5	−0.465	−2.196; 1.368	0.64
D RPA	5.6/2.1	5.8/2.1	−0.469	−1.418; 0.88	0.64
D LPA	5.3/2.3	5.7/2.3	−0.704	−1.631; 0.783	0.49
D AscAo	7.9/2.5	8.5/2.5	−0.76	−1.818; 0.817	0.45

(Continued)

Table 2 (continued)

Measurement area	M/SD		t	CI [95%]	p^1
	1 group*	2 group*			
D BCT	4.8/1	5.3/1.2	−1.649	−1.117; 0.109	0.1
D LCCA	3.7/0.9	3.9/1	−1.13	−0.822; 0.229	0.26
D LSA	3.6/1	3.9/1	−1.104	−0.815; 0.236	0.27
D DesAo	6.3/1.6	6.8/1.7	−1.021	−1.307; 0.425	0.31

Notes: 1 group*: CT-scan; 2 group*: 3D-model. [1]Signifies a statistically significant value ($p < 0.05$). D, diameter; PA pulmonary artery; RPA, LPA, right and left pulmonary arteries; AscAo, ascending aorta; BCT, brachiocephalic trunk, LCCA, left common carotid artery; LSA, subclavian artery; DesAo, descending aorta.

Table 3: Results of statistical analysis of comparison of measurements (Mann–Whitney U-test)

Measurement area	M/SD	Md	U	Z	p^1
Heart length	61.4/12.03	59.3 [54.7; 66.1]	391	−0.459	0.65
Heart width	43.1/8.38	41.6 [37.8; 46.6]	418.5	−0.031	0.98
D AoArch	6.8/3.55	6.1 [4.6; 7.4]	379.5	−0.638	0.52

Notes: [1]Signifies a statistically significant value ($p < 0.05$). D, diameter; AoArch, aortic arch.

4 Discussion

In our study, we compared measurements of similar areas of the heart and great vessels on a printed model and on tomography images of the same patient. The main indicators of the advantages of 3D printing in our study were the accuracy of printing, the correlation between a 3D model and the actual size of an organ, and also spatial relationship of anatomical formations.

3D printing technology proved to be a promising technique in the medical industry, but it is still at the stage of research, development, and implementation in all areas of surgery [15,35]. Application of this method in cardiac surgery, especially in pediatrics, has just begun to be widely used but is already helping to improve the outcomes of reconstructive procedures [16,36,37]. An interesting study compared four programs with different segmentation algorithms and evaluated the results by measuring the same zones on models [38]. Statistically significant discrepancies and unsatisfactory results were found in the comparison of volume and surface area for the final models of a mandible and a tumor. In addition, the study showed that the minimal time spent on the preparation of a model for printing was 2 h and a maximum of 4.6 h, depending on the program used.

According to the results of our study, there were no statistically significant deviations of control measurements on a printed model of the heart, compared with measurements on computed tomography. To determine the possibility of using printed models for the purpose of preoperative preparation, assessment of accuracy, and information content in our study, measurements of similar anatomical zones and formations were performed on 3D models and tomography images in 29 children. The results confirm the required accuracy of the printed models and the possibility of using 3D printing to achieve goals when planning a surgery. In addition, the developed algorithm meets the requirements of preprint processing of computed tomography data. Along with this, given the fact that the time to prepare the model for printing has significantly decreased and ranges from 2 to 10 min, this new algorithm has an undeniable advantage.

In some cases, we performed intraoperative measurements of the same anatomical regions (Fig. 3). The presented images show a high level of similarity; this can be used for simulation surgeries as part of preoperative preparation.
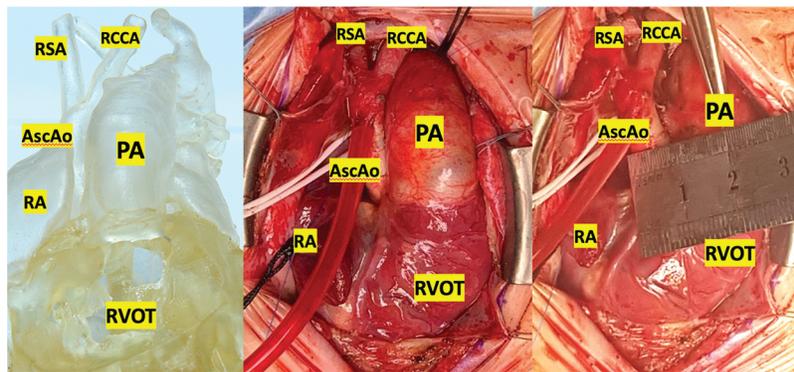
Figure 3: Comparison of the printed model with intraoperative anatomy of the heart and great vessels in a child with the interrupted aortic arch (type C). Notes: RVOT, right ventricle output tract; PA, pulmonary artery; RA, right atrium; AscAo, ascending aorta; RCCA, right common carotid artery; RSA, right subclavian artery

3D models have been successfully used to simulate transcatheter aortic and mitral valve replacement, to predict the size of the annulus and the type of leaflet resection/correction [22]. One study compared the sizes of 3D-printed mitral valves with prolapse with intraoperative data [24]. The differences were moderate. In hypertrophic cardiomyopathy, a thorough assessment of the anatomy of the left ventricle before surgical myectomy is of paramount importance [39,40].

Most of the works are related to adult cardiac surgery. In international databases, literature reviews and case reports are predominantly published. The use of 3D modeling in pediatric cardiac surgery has not been studied enough. In contrast to publications on adult cardiac surgery, in papers on the use of 3D printing in pediatric cardiac surgery, the authors focus on the advantages of imaging for cardiac defects.

As a part of this work, eight simulation operations were performed on printed models of the heart using a silicone-like photopolymer in children with ventricular septal defect (Figs. 4–7). A seemingly simple procedure might also be challenging. One of the inconveniences when performing VSD repair is the formation of a patch that is geometrically comparable to the defect before it is sewn. For example, if you select a patch larger than the defect, in some cases it is not possible to reduce it. In this case, a surgeon has to plicate the patch so that it does not protrude or close the defect again. Therefore, in such cases, in addition to closing the defect, we determined the required size of the patch and its shape in each case. These calculations were monitored in the operating room. In all cases, the application of the formed patch according to the preliminary measurements and geometric shape confirmed compliance. This fact suggests that pre-calculations of the patch in the planned VSD repair with complex localization will improve the outcomes of the repair because operating time and the risks of complications will decrease. This approach must be implemented for all types of CHD, especially with the complex anatomy of the defect.

It should be noted that the number of centers that have implemented 3D printing technology in clinical practice, especially in cardiovascular surgery, is increasing every year. Planning a surgery, and studying features of the anatomy of the pathologies on the printed model is becoming increasingly relevant and adds to better outcomes of surgical treatment [25,27,41–43]. Application of this method in pediatric cardiac surgery will allow evaluation of intracardiac anatomy, extracardiac defects, isolated vascular anomalies, and complex heart defects such as aortopulmonary collaterals in patients with pulmonary atresia [42–44]. 3D models provide a detailed view of the collaterals, which is extremely informative in preoperative planning. In congenital heart defects, surgical repair, since it is usually necessary in the neonatal period or in infancy, has paramount importance, since the effect of a surgery directly determines the hemodynamic effect in a patient.
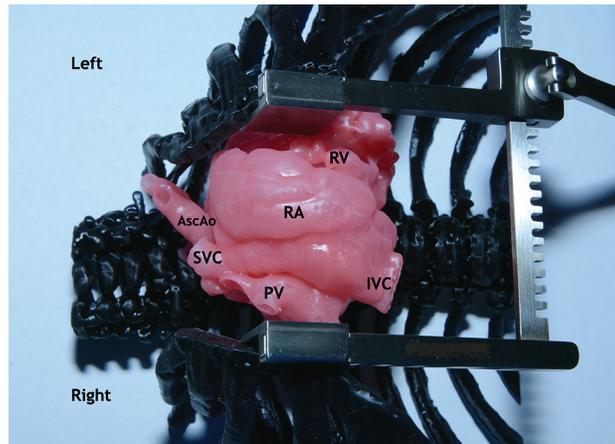
Figure 4: Silicone-printed 3D model of a child's heart with a VSD. Modeling of the surgical field: The chest is dissected and expanded with a retractor. Orthotopic arrangement of the heart model. Abbreviation: RV, right ventricle; RA, right atrium; PV, right pulmonary veins; IVC, inferior vena cava; SVC, superior vena cava; VSD, ventricular septum defect; AscAo, ascending aorta
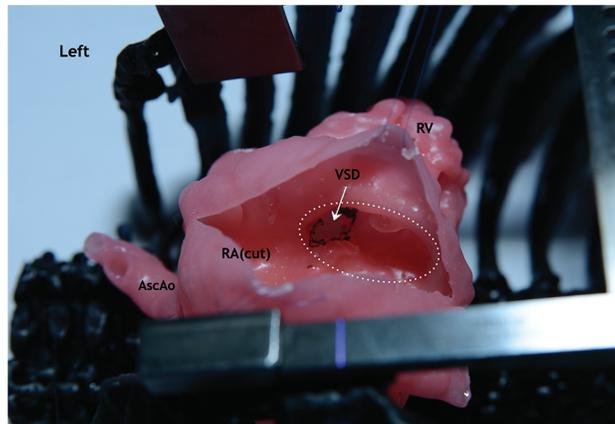

Figure 5: Silicone-printed 3D model of a child's heart with a VSD. The right atrium is cut parallel to the terminal sulcus. Operation view: VSD is visualized through the fibrous ring of the tricuspid valve (circle with white dotted line). Abbreviation: RV, right ventricle; RA, right atrium; VSD, ventricular septum defect; AscAo, ascending aorta

4.1 Limitations

A single-center study was performed, but a larger sample size is required to validate the statistical power of the outcomes. The main task was to evaluate the effectiveness of the use of 3D printing techniques in pediatric cardiac surgery based on the algorithm creating the model, which is directly related to the possibility of practical application of this method. The currently available capabilities of this technology cope successfully with the first task. And the second task leaves a lot of unresolved issues. Performing a simulated surgery on a 3D-printed model could be a challenging task because it is necessary for the material to be similar to human soft tissues (in our case, muscle tissue, and blood vessels). Currently, there are only a few such materials and they can only be used on specialized printers. In addition, they are not widely available. For widespread use, there are only a few options for soft polymers similar to

silicone. Given these technical limitations, the possibility of using 3D printing to simulate surgery on a printed model is significantly complicated.
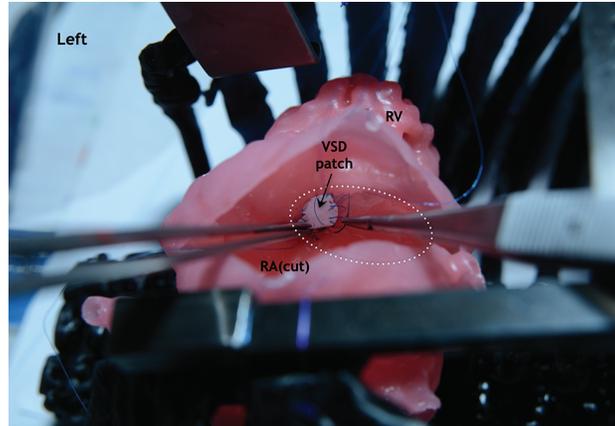

Figure 6: Silicone-printed 3D model of a child's heart with a VSD. Operation view through the right atrium. Stages of simulating a defect closure with use a synthetic patch. The fibrous ring of the tricuspid valve is visualized (circle with white dotted line). Abbreviation: RV, right ventricle; RA, right atrium; VSD, ventricular septum defect
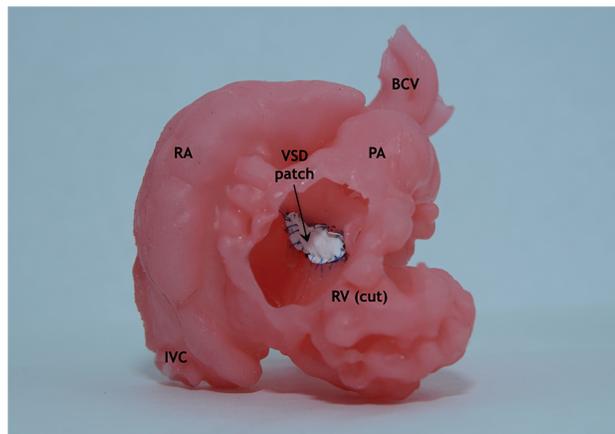

Figure 7: Final view through the dissected right ventricle. Silicone-printed 3D model of a child's heart with a VSD. The defect is closed with use a synthetic patch. Abbreviation: RV, right ventricle; RA, right atrium; IVC, inferior vena cava; PA, pulmonary artery; VSD, ventricular septum defect; BCV, brachiocephalic vessels

In addition, we consider it important to continue the improvement of the program with the developed preprint processing algorithm and believe it is necessary to ensure the availability of this program for medical specialists. Besides it is still the issue that the software or the algorithms have not yet been approved for medical or for clinical use.

5 Conclusions

3D-printed model of the heart and great vessels in patients with congenital heart disease provides an accurate preoperative assessment of the anatomy of the disease in each individual case, which is

confirmed by the results of this work. It is possible to evaluate spatial relations, intracardiac defects, and abnormalities. Furthermore, it may reduce the risks of complications, duration of extracorporeal circulation, and surgery. In addition, the use of soft and flexible materials gives a chance to undertake the possible type of procedure on a printed 3D model in each individual case and evaluate its effectiveness.

The advantages of the newly developed preprinting algorithm preparation were demonstrated. The new algorithm greatly simplifies and speeds up the preparation of a 3D model for printing, while maintaining high accuracy and detail. The new algorithm has several important advantages over currently available programs: the segmentation time is reduced from several hours to several minutes (2–10 min); the program is adapted for work by unskilled specialists in the field of programming; automatic segmentation results in a model with a high level of fit, low noise and artifacts (this significantly reduces or eliminates the need for additional manual refinement). Such possibilities help to come up with an individual preliminary plan for surgical repair of complex congenital heart disease, anticipate possible issues, and determine the optimal treatment tactics that may significantly improve outcomes in our daily practice.

Author Contributions: Vitaliy Suvorov has made substantial contributions to the intellectual content of an article in terms of the conception, drafting, and revising of the work, analysis, and interpretation of the data, the final approval of the version to be published. Olga Loboda has made substantial contributions to the intellectual content of an article in terms of the conception, drafting of the article and revising of the work, the final approval of the version to be published. Igor Kulczycki developed an algorithm for prepress processing of tomography data, has made a significant contribution to the content of the article in terms of writing the work, as well as data processing, the final approval of the version to be published. Maria Balakina has made substantial contributions to the content of an article in terms of the drafting, and revising of the work and the acquisition of the data, the final approval of the version to be published.

Availability of Data and Materials: The datasets generated during and/or analyzed during the current study are available from the corresponding author on reasonable request.

Ethics Approval: Our study was approved by the Ethics Committee (the Local Ethics Committee at the Saint Petersburg State Pediatric Medical University, No. 18/03 27.10.2022). Parents of patients were informed about the use of examination and treatment data in scientific research and gave their consent.

Conflicts of Interest: The authors declare that they have no conflicts of interest to report regarding the present study.

References

1. Martelli, N., Serrano, C., van den Brink, H., Pineau, J., Prognon, P. et al. (2016). Advantages and disadvantages of 3-dimensional printing in surgery: A systematic review. *Surgery, 159,* 1485–1500. https://doi.org/10.1016/j.surg.2015.12.017
2. Kosulin, A. V., Elyakin, D. V. (2017). The use of a physical 3D model as a reference object in the surgical treatment of congenital kyphoscoliosis. *Pediatrician, 8,* M163–M164.
3. Jones, T. W., Seckeler, M. D. (2017). Use of 3D models of vascular rings and slings to improve resident education. *Congenital Heart Disease, 12(5),* 578–582. https://doi.org/10.1111/chd.12486
4. Shenaq, D. S., Matros, E. (2018). Virtual planning and navigational technology in reconstructive surgery. *The Journal of Surgical Oncology, 118(5),* 845–852. https://doi.org/10.1002/jso.25255

5. Ghai, S., Sharma, Y., Jain, N., Satpathy, M., Pillai, A. K. (2018). Use of 3-D printing technologies in craniomaxillofacial surgery: A review. *Oral and Maxillofacial Surgery, 22(3),* 249–259. https://doi.org/10.1007/s10006-018-0704-z

6. Fan, B., Chen, H., Sun, Y. J., Wang, B. F., Che, L. et al. (2017). Clinical effects of 3-D printing-assisted personalized reconstructive surgery for blowout orbital fractures. *Graefe's Archive for Clinical and Experimental Ophthalmology, 255(10),* 2051–2057. https://doi.org/10.1007/s00417-017-3766-y

7. Li, C., Cheung, T. F., Fan, V. C., Sin, K. M., Wong, C. W. et al. (2017). Applications of three-dimensional printing in surgery. *Surgical Innovation, 24(1),* 82–88. https://doi.org/10.1177/1553350616681889

8. Bauermeister, A. J., Zuriarrain, A., Newman, M. I. (2016). Three-dimensional printing in plastic and reconstructive surgery: A systematic review. *Annals of Plastic Surgery, 77,* 569–576. https://doi.org/10.1097/SAP.0000000000000671

9. Soon, D. S., Chae, M. P., Pilgrim, C. H., Rozen, W. M., Spychal, R. T. et al. (2016). 3D haptic modelling for preoperative planning of hepatic resection: A systematic review. *Annals of Medicine and Surgery, 10,* 1–7. https://doi.org/10.1016/j.amsu.2016.07.002

10. Patzelt, S. B., Spies, B. C., Kohal, R. J. (2015). CAD/CAM-fabricated implant-supported restorations: A systematic review. *Clinical Oral Implants Research, 26,* 77–85. https://doi.org/10.1111/clr.12633

11. Bidra, A. S., Taylor, T. D., Agar, J. R. (2013). Computer-aided technology for fabricating complete dentures: Systematic review of historical background, current status, and future perspectives. *The Journal of Prosthetic Dentistry, 109,* 361–366. https://doi.org/10.1016/S0022-3913(13)60318-2

12. Tack, P., Victor, J., Gemmel, P., Annemans, L. (2016). 3D-printing techniques in a medical setting: A systematic literature review. *BioMedical Engineering OnLine, 15(1),* 115. https://doi.org/10.1186/s12938-016-0236-4

13. Boll, L. F. C., Rodrigues, G. O., Rodrigues, C. G., Bertollo, F. L., Irigoyen, M. C. et al. (2019). Using a 3D printer in cardiac valve surgery: A systematic review. *Revista da Associação Médica Brasileira, 65(6),* 818–824. https://doi.org/10.1590/1806-9282.65.6.818

14. Wang, J. Z., Xiong, N. Y., Zhao, L. Z., Hu, J. T., Kong, D. C. et al. (2018). Review fantastic medical implications of 3D-printing in liver surgeries, liver regeneration, liver transplantation and drug hepatotoxicity testing: A review. *International Journal of Surgery, 56,* 1–6. https://doi.org/10.1016/j.ijsu.2018.06.004

15. Yoo, S. J., Thabit, O., Kim, E. K., Ide, H., Yim, D. et al. (2016). 3D printing in medicine of congenital heart diseases. *3D Printing in Medicine, 2(1),* 3. https://doi.org/10.1186/s41205-016-0004-x

16. Schmauss, D., Juchem, G., Weber, S., Gerber, N., Hagl, C. et al. (2014). Three-dimensional printing for perioperative planning of complex aortic arch surgery. *The Annals of Thoracic Surgery, 97,* 2160–2163. https://doi.org/10.1016/j.athoracsur.2014.02.011

17. Zadpoor, A. A., Malda, J. (2017). Additive manufacturing of biomaterials, tissues, and organs. *Annals of Biomedical Engineering, 45,* 1–11. https://doi.org/10.1007/s10439-016-1719-y

18. Suvorov, V. V., Zaytsev, V. V., Kupatadze, D. D., Krivoshchekov, E. V., Loboda, O. S. et al. (2020). 3D printing technology in planning of surgical strategy for complex congenital heart defects. *Russian Journal of Cardiology and Cardiovascular Surgery, 13(4),* 294–298. https://doi.org/10.17116/kardio202013041294

19. Yao, X. W., Ai, K., Li, Y. (2022). Presurgical planning of 3D printing for a large abdominal pheochromocytoma and paraganglioma. *Urology, 165,* 356–358. https://doi.org/10.1016/j.urology.2022.04.033

20. Valverde, I. (2017). Three-dimensional printed cardiac models: Applications in the field of medical education, cardiovascular surgery, and structural heart interventions. *Revista Española de Cardiología (English Edition), 70(4),* 282–291. https://doi.org/10.1016/j.rec.2017.01.012

21. Nocerino, E., Remondino, F., Uccheddu, F., Gallo, M., Gerosa, G. (2016). 3D modelling and rapid prototyping for cardiovascular surgical planning—Two case studies. *The International Archives of the Photogrammetry, Remote Sensing and Spatial Information Sciences, XLI-B5,* 887–893. https://doi.org/10.5194/isprs-archives-XLI-B5-887-2016

22. Wang, C., Zhang, L., Qin, T., Xi, Z., Sun, L. et al. (2020). 3D printing in adult cardiovascular surgery and interventions: A systematic review. *The Journal of Thoracic Disease, 12(6),* 3227–3237. https://doi.org/10.21037/jtd-20-455

23. Wang, D. D., Qian, Z., Vukicevic, M., Engelhardt, S., Kheradvar, A. et al. (2021). 3D printing, computational modeling, and artificial intelligence for structural heart disease. *Journal of the American College of Cardiology: Cardiovascular Imaging, 14(1),* 41–60. https://doi.org/10.1016/j.jcmg.2019.12.022

24. Shirakawa, T., Yoshitatsu, M., Koyama, Y., Mizoguchi, H., Toda, K. et al. (2018). 3D-printed aortic stenosis model with fragile and crushable calcifications for off-the-job training and surgical simulation. *The Multimedia Manual of Cardio-Thoracic Surgery.* https://doi.org/10.1510/mmcts.2018.018

25. Zavadovsky, K. W., Krivoshekov, E. V., Brasovsky, K. S., Lezhnev, A. A., Mochula, A. V. et al. (2018). 3D printing in preoperative assessment of cardiac anatomy in patient with congenital ventricular septal defect and double-chambered right ventricle. *Russian Electronic Journal of Radiology, 8(1),* 194–201. https://doi.org/10.21569/2222-7415-2018-8-1-194-201

26. Goo, H. W., Park, S. J., Yoo, S. J. (2020). Advanced medical use of three-dimensional imaging in congenital heart disease: Augmented reality, mixed reality, virtual reality, and three-dimensional printing. *The Korean Journal of Radiology, 21,* 133–145. https://doi.org/10.3348/kjr.2019.0625

27. Korchagina, D. O., Badurov, R. B., Suvorov, V. V., Starchik, D. A. (2022). 3D printing for planning of surgery in a newborn with aortic arch pathology. *Russian Journal of Cardiology and Cardiovascular Surgery, 15(1),* 85–90. https://doi.org/10.17116/kardio20221501185

28. Ardila, C. M., González-Arroyave, D., Zuluaga-Gómez, M. (2023). Efficacy of three-dimensional models for medical education: A systematic scoping review of randomized clinical trials. *Heliyon, 9(2),* e13395. https://doi.org/10.1016/j.heliyon.2023.e13395

29. Perens, G., Yoshida, T., Finn, J. P. (2022). A rare case of concordant atrioventricular connection to L-looped ventricles in situs solitus: 4-dimensional magnetic resonance imaging and 3D printing. *Congenital Heart Disease, 17(4),* 387–392. https://doi.org/10.32604/chd.2022.021233

30. Yuan, Q., Chen, X., Zhai, J., Chen, Y., Liu, Q. et al. (2021). Application of 3D modeling and fusion technology of medical image data in image teaching. *BMC Medical Education, 21,* 194. https://doi.org/10.1186/s12909-021-02620-z

31. OpenCv. https://opencv.org

32. Marching Cubes 3d Tutorial (2018). BorisTheBrave.Com. https://www.boristhebrave.com/2018/04/15/marching-cubes-3d-tutorial

33. Autodesk 3ds max. Wikipedia. https://ru.wikipedia.org/wiki/Autodesk_3ds_Max

34. Kholmatova, K. K., Kharkova, O. A., Grjibovski, A. M. (2016). Experimental studies in medicine and public health: Planning, data analysis, interpretation of results. *Ekologiya Cheloveka (Human Ecology), 23(11),* 50–58. https://doi.org/10.33396/1728-0869-2016-11-50-58

35. Mulford, J. S., Babazadeh, S., Mackay, N. (2016). Three-dimensional printing in orthopaedic surgery: Review of current and future applications. *ANZ Journal of Surgery, 86,* 648–653. https://doi.org/10.1111/ans.13533

36. Jones, D. B., Sung, R., Weinberg, C., Korelitz, T., Andrews, R. (2016). Three-dimensional modeling may improve surgical education and clinical practice. *Surgical Innovation, 23(2),* 189–195. https://doi.org/10.1177/1553350615607641

37. Illmann, C. F., Ghadiry-Tavi, R., Hosking, M., Harris, K. C. (2020). Utility of 3D printed cardiac models in congenital heart disease: A scoping review. *Heart, 106(21),* 1631–1637. https://doi.org/10.1136/heartjnl-2020-316943

38. Fogarasi, M., Coburn, J. C., Ripley, B. (2022). Algorithms used in medical image segmentation for 3D printing and how to understand and quantify their performance. *3D Printing in Medicine, 8(1),* 18. https://doi.org/10.1186/s41205-022-00145-9

39. Andrushchuk, U., Adzintsou, V., Nevyglas, A., Model, H. (2018). Virtual and real septal myectomy using 3-dimensional printed models. *Interactive Cardiovascular and Thoracic Surgery, 26,* 881–882. https://doi.org/10.1093/icvts/ivx410

40. Hermsen, J. L., Burke, T. M., Seslar, S. P., Owens, D. S., Ripley, B. A. et al. (2017). Scan, plan, print, practice, perform: Development and use of a patient-specific 3-dimensional printed model in adult cardiac surgery. *The Journal of Thoracic and Cardiovascular Surgery, 153,* 132–140. https://doi.org/10.1016/j.jtcvs.2016.08.007

41. Kiraly, L., Tofeig, M., Jha, N. K., Talo, H. (2016). Three-dimensional printed prototypes refine the anatomy of post-modified Norwood-1 complex aortic arch obstruction and allow presurgical simulation of the repair. *Interactive Cardiovascular and Thoracic Surgery, 22,* 238–240. https://doi.org/10.1093/icvts/ivv320

42. White, S. C., Sedler, J., Jones, T. W., Seckeler, M. (2018). Utility of three-dimensional models in resident education on simple and complex intracardiac congenital heart defects. *Congenital Heart Disease, 13(6),* 1045–1049. https://doi.org/10.1111/chd.12673

43. Averkin, I. I., Grehov, E. V., Pervunina, T. M., Komlichenko, E. V., Vasichkina, E. S. et al. (2022). 3D-printing in preoperative planning in neonates with complex congenital heart defects. *The Journal of Maternal-Fetal & Neonatal Medicine, 35(10),* 2020–2024. https://doi.org/10.1080/14767058.2020.1771691

44. Nam, J. G., Lee, W., Jeong, B., Park, E. A., Lim, J. Y. et al. (2021). Three-dimensional printing of congenital heart disease models for cardiac surgery simulation: Evaluation of surgical skill improvement among inexperienced cardiothoracic surgeons. *The Korean Journal of Radiology, 22(5),* 706–713. https://doi.org/10.3348/kjr.2020.0682